Published in final edited form as:
Int J Radiat Oncol Biol Phys. 2007 March 15; 67(4): 1179–1186.

Correlation of Radiation Response with Tumor Oxygenation in the Dunning Prostate R3327-AT1 Tumor

Vincent A. Bourke, Ph.D.[a,#], **Dawen Zhao, MD, Ph.D.**[a], **Joseph Gilio, Ph.D.**[b], **Cheng-Hui Chang, Ph.D.**[b], **Lan Jiang, Ph.D.**[a], **Eric W. Hahn, Ph.D.**[a], and **Ralph P. Mason, Ph.D.**[a]

a *Department of Radiology, University of Texas Southwestern Medical Center, Dallas, TX*

b *Department of Radiation Oncology, University of Texas Southwestern Medical Center, Dallas, TX*

Abstract

Purpose— It is widely recognized that tumor oxygenation may modulate the efficacy of radiation therapy. Previously, a correlation was established between pre-treatment oxygenation and growth delay following radiation therapy in the slower growing HI subline of the R3327 Dunning prostate tumor. We have now investigated application to the more hypoxic, faster growing AT1 subline.

Methods and Materials— Dunning prostate R3327-AT1 tumors growing on Copenhagen rats were administered 30 Gy of X-ray radiation either with or without oxygen inhalation. Tumor oxygenation was sampled by ^{19}F nuclear magnetic resonance echo planar imaging relaxometry (*FREDOM*) of the reporter molecule hexafluorobenzene, no more than 24 hours prior to irradiation.

Results— Large tumors (>3.0 cm^3) exhibited significantly greater hypoxic fractions and lower mean pO_2 than their smaller counterparts (<1.5 cm^3). However unlike the R3327-HI subline, large AT1 tumors generally did not respond to oxygen inhalation in terms of altered hypoxic fraction or response to irradiation. While the tumors did not respond to oxygen inhalation, each tumor had a different pO_2 and there was a clear trend between level of oxygenation at time of irradiation and tumor growth delay, with considerably better outcome when mean pO_2 > 10 torr. The comparatively small baseline hypoxic fraction in the group of small tumors was virtually eliminated by breathing oxygen and the growth rate was significantly reduced for tumors on rats breathing oxygen during irradiation.

Conclusions— These results further validate the usefulness of NMR oximetry as a predictor of response to radiation therapy.

Keywords

prostate tumor; oxygen; hypoxia; radiation response; fluorine NMR

INTRODUCTION

For more than 50 years it has been recognized that tumor oxygenation may significantly modulate the efficacy of various therapeutic interventions, particularly radiation therapy [1–7]. Hypoxic tumors are characteristically more resistant to radiotherapy, and the ability to sample

Corresponding Author: Ralph P. Mason, Ph.D., CSci., CChem., University of Texas Southwestern Medical Center at Dallas, 5523 Harry Hines, Dallas Texas, Phone: (214) 648-8926, Fax: (214) 648-4538, E-mail: ralph.mason@utsouthwestern.edu.
[#]Currently, Department of Nuclear and Radiological Engineering, University of Florida, Gainesville, FL 32611

pretreatment oxygenation may prove to be a useful predictor of therapeutic outcome. In principle, there are many techniques available for the manipulation of intratumoral oxygen tension for therapeutic advantage, such as inhalation of hyperoxic gases. However, few have shown significant improvement in clinical outcome and it is thought that this may be due to the inability, hitherto, to identify those patients, who would benefit most [8]. Thus, the ability to dynamically sample the oxygenation status of tumors, and monitor the response to adjuvant intervention could be very valuable. As reviewed [9–12], various methods have been developed for probing tumor oxygenation including hypoxia reporter agents, polarographic electrodes, fiber optic probes, NIR spectroscopy, and various NMR techniques, but most are either highly invasive, lack spatial resolution or lack the ability to dynamically and quantitatively sample the response to intervention.

We have developed an approach to dynamically sample tumor oxygen tension at multiple locations simultaneously: *FREDOM* (Fluorocarbon Relaxometry using Echo planar imaging for Dynamic Oxygen Mapping) MRI, following direct intratumoral injection of the reporter molecule hexafluorobenzene (HFB) [9]. We have applied this method to explore tumor pO_2 in various rat prostate and breast tumors and human tumor xenografts with respect to interventions [9, 13–17]. We also showed that response to single high dose radiation therapy in the slower Dunning Prostate R3327-HI was related to pO_2 [18]. Inhalation of oxygen during 30 Gy irradiation resulted in enhanced growth delay in larger HI tumors (>3.5 cm^3), but had no effect on smaller tumors (<2 cm^3). It was found that the larger HI tumors have a high baseline hypoxic fraction (HF_{10} >80%), but this could be effectively eliminated by breathing hyperoxic gas (HF_{10} ~20% with oxygen breathing). By contrast smaller tumors showed minimal baseline hypoxia (HF_5 ~20%) and although this was diminished, it was relatively inconsequential. We have also assessed differential characteristic responses to hyperoxic gas breathing in other sublines of the Dunning prostate R3327 [14, 15]. Most notably, the faster growing AT1 tumors (VDT ~ 5 days) were significantly less well oxygenated than size matched HI tumors, and unlike the HI subline, the critical initially hypoxic regions responded little to oxygen inhalation [15]. It thus appeared that the AT1 subline should provide an important extension to further validate the utility of oxygen tension measurements for predicting response to irradiation. In an initial test, we examined the growth delay in tumors on rats breathing oxygen or air during irradiation. We then expanded the investigation to include pO_2 measurements based on the *FREDOM* technique. Since hypoxic fraction was previously observed to increase with the size of the tumor [15], we investigated cohorts of small and large AT1 tumors, while rats breathed air or oxygen.

METHODS AND MATERIALS

Investigations were conducted in accordance with accepted ethical and humane practices, and approved in advance by the UT Southwestern Medical Center Institutional Animal Care and Use Committee (IACUC).

Tumor Model

Syngeneic Dunning prostate R3327-AT1 carcinomas, a fast growing, poorly differentiated subline with a potential volume doubling time (T_{pot}) of 4.4 days, were originally obtained from Dr. J. T. Isaacs, of Johns Hopkins University and provided to us by Dr. Peter Peschke of the German Cancer Research Center (DKFZ), Heidelberg, Germany. For the preliminary study, tumors were implanted in surgically prepared foreback pedicles of 14 adult male Copenhagen rats (~250 g, Harlan, Indianapolis, IN) [19]. In the preliminary study, when the tumors reached a suitable size (0.9 to 2.8 cm^3), the rats were divided into three groups for therapy: Group 1: control sham irradiated tumors (no treatment, n=4; mean size 1.9 ± 1.0 (SD) cm^3), Group 2-air: rats breathing air during tumor irradiation (n=5; mean tumor size 1.6 ± 0.7 cm^3), and Group

2-O_2: rats breathing oxygen during tumor irradiation (n=5, mean tumor size = 1.5 ± 0.3 cm^3). For the more extensive second study 28 tumors were implanted as before. In this case, the rats were divided into five groups: Group 3: control rats (no treatment, n=6), Groups 4-air (n=5) and 4-O_2 (n=5) rats with large tumors (>3.0 cm^3, mean size at treatment = 4.3 ± 0.4 cm^3), and Groups 5-air (n=6) and 5-O_2 (n=6) rats with small tumors (<1.25 cm^3, mean size at treatment = 0.8 ± 0.1 cm^3). Groups breathed air or oxygen, respectively, as designated during irradiation. Tumor diameter was measured with calipers in three orthogonal axes beginning seven days after implantation, and continuing every 3-7 days until sacrifice. Tumor volume was calculated as V=(π/6)**abc*, where *a*, *b*, and *c* are the three orthogonal diameters. In some cases, tumor volume was estimated for a given day by interpolating between actual measured sizes. For each group, mean tumor size on a given day was estimated using measurements acquired over three day intervals (*e.g.*, day 2 = days 1–3, day 5= days 4–6).

Tumor Oximetry (Groups 4 and 5)

In approximately half of the animals which were irradiated (Large, n=6; Small, n=6), NMR oximetry measurements were obtained within 24 h prior to irradiation. Each rat was sedated with 200 μl ketamine hydrochloride (100 mg/kg, Aveco, Fort Dodge, IA) and maintained under general anesthesia [1.2 L/min, air+1.2% isoflurane (Baxter International Inc., Deerfield, IL)]. The animal was positioned on its side on a cradle, and body temperature was maintained with a warm water blanket. As previously described [9], hexafluorobenzene (50 μl; Lancaster, Gainesville, FL) was deoxygenated by bubbling with CO_2 for 5 minutes prior to use, and then was injected using a Hamilton syringe (Reno, NV) and a fine sharp 32G needle. To ensure representative sampling of intratumoral oxygenation, the HFB was deposited along three diverging tracks encompassing both central and peripheral regions in a central plane coronal to the rat's body. It is important to note that the AT1 subline tumors do not develop a central necrosis. Thus, the oxygenation data are obtained from viable tissues.

NMR imaging was performed on representative rats from Groups 4 and 5 using a 4.7 T horizontal bore NMR system (Varian Inc., Palo Alto, CA). A tunable ($^1H/^{19}F$) single turn solenoid volume coil (either 2 or 3.5 cm, size matched to tumor diameter) was placed around the tumor bearing pedicle, and conventional spin echo scout images were obtained for both ^1H (200.1 MHz) and ^{19}F (188.3 MHz) to reveal HFB distribution within the tumor.

^{19}F pulse burst saturation recovery echo planar imaging (EPI) relaxometry of the HFB (*FREDOM*) was used to measure pO_2, while rats breathed air or with respect to breathing air followed by oxygen. Fourteen delay times in the range 150 ms to 90 s were used to generate the relaxation data with in plane resolution 1.25 mm and 20 mm slice thickness as described in detail previously [9]. Two rats from each Group were examined while breathing air only (four consecutive pO_2 maps obtained over 24 mins). Four rats from each group were examined 4 times while breathing air followed by 4 consecutive measurements during the first 24 minutes following switching to breathing oxygen. Spin lattice relaxation rates (R1=1/T1) were estimated on a voxel by voxel basis and pO_2 calculated using the relationship pO_2 (torr)= [(R1-0.0835)/0.001876] [9]. Since even noise can give an R1 curve fit, voxels were rejected if T1 error >2.5 s, or ratio T1 error/T1 >50%. We also required that voxels give reliable pO_2 measurements throughout the series of measurements: thus, each voxel provided four or eight consecutive pO_2 measurements, which were deemed acceptable on the basis of the T1 error acceptance criteria.

Radiation Treatment (Groups 2, 4 and 5)

Within 24 hours of the NMR scans, the animals were sedated with 200 μl ketamine hydrochloride (100 mg/kg I.P.) and then irradiated with single dose of 30 Gy (2 Gy/min) using a 4MV Varian Clinac 4/100 linear accelerator under general gaseous anesthesia (1.2 L/min,

gas +1.2% isoflurane) [20]. Tissue equivalent bolus (1 cm thick) was placed over the tumor during irradiation to ensure dose uniformity. The rats in Group 2-air (n=5), 4-air (n=5) and 5-air (n=6) breathed air during irradiation, while those in Group 2-O_2 (n=5), 4-O_2 (n=5) and 5-O_2 (n=6) breathed oxygen for 30 mins prior to irradiation and during irradiation. The rats examined by NMR on the previous day breathed the corresponding gas during irradiation. Tumor size was normalized to the initial size on the day of irradiation. Treatment response was evaluated based on reduction in the tumor growth rate and time to double in volume (T2) post irradiation. If a tumor failed to double in volume by the time of sacrifice, the day of sacrifice was taken as T2, though this may represent an underestimate for responsive tumors.

Statistical Analysis

The statistical significance of differences in mean tumor size, and changes in oxygenation, was assessed using an analysis of variance (ANOVA) based on Fisher's protected least significant difference (PLSD). Hypoxic fractions (HF_{10} < 10 Torr) were calculated for each tumor by counting the number of hypoxic voxels versus total number of measured voxels in the respective pO_2 map. Animals were excluded from hypoxic fraction analysis, if the associated pO_2 map did not contain at least ten acceptable voxels. Kaplan-Meier hazard statistics were applied to test the significance of differences in T_2, the time to double the initial treated tumor volume on day 0 (V_0).

RESULTS

In our preliminary studies there was a significant growth delay by day 12 following irradiation ($p<0.05$) for rats breathing air or oxygen compared with controls and the relative mean tumor sizes were 3.7±0.9 cm^3 (Group 1 (control)), 2.2±0.9 cm^3 (Group 2-air) and 2.0± 0.6 cm^3 (Group 2-O_2). No differences were found between breathing air or oxygen (Fig. 1A). On Day 32 Group 2-air had a mean relative volume of 4.9 ±3.5 cm^3 compared with a volume of 3.4 ±2.9 cm^3 for Group 2-O_2. The lack of difference may be attributed to the broad range of responses related to the range of initial tumor sizes and levels of oxygenation (Fig. 1B). Thus, we undertook a more detailed second investigation with tumors divided into Groups based on size (large and small) and with oxygen tension measurements in representative tumors.

Overlay of the ^{19}F and ^{1}H NMR images shows distribution of the reporter molecule HFB (Fig. 2). Between 300 and 600 voxels indicated ^{19}F signal in the echo planar images and provided relaxation curves in the *FREDOM* measurements. Applying the acceptance criteria caused rejection of 50 to 75% of these data voxels based on excessive T1 error (poor quality curve fits). Applying the further requirement that voxels give consistently acceptable T1 values throughout the series of measurements caused further voxels to be rejected. For both air and oxygen breathing groups one tumor for each size provided such poor quality data that fewer than 10 voxels remained. These tumors are included in the consideration of tumor growth delay in Table 2, but are omitted from consideration of pO_2 measurement (Table 1). For the remaining tumors between 12 and 102 individual pO_2 measurements were considered reliable in each AT1 tumor and representative maps are shown for a large AT1 tumor in Figure 2A, B, and C. Here, 51 voxels were acceptable indicating a mean (±SE) baseline pO_2 = 0.1 ± 1.8 torr (mean baseline HF_{10} = 87.3 ± 1.8%) during the initial 6 minute air inhalation period, which was found to be stable over the next 18 mins. A modest, but significant ($p<0.01$) increase was observed by the last six minutes of oxygen inhalation (Fig. 2C), though mean HF_{10} remained unchanged. Large AT1 tumors were significantly more hypoxic than small ones, and hypoxic fractions generally did not respond significantly to oxygen inhalation (Figs. 2, 3, and Table 1). The small tumors were initially better oxygenated, and showed much greater response to oxygen inhalation (Fig. 2D, E, F).

The influence of oxygen breathing on response to radiation was evaluated as change in the tumor growth rate, based on mean tumor size at various times following irradiation, and T_2, the time to double the initial tumor size on the day of treatment (Table 2). Each tumor was normalized to V_o, its initial size on the day of irradiation. Each tumor in the untreated control group was normalized to its size on post-implantation day 13, the day on which the control group reached a mean size of about 1 cm^3. Untreated controls (Group 3) were allowed to grow until the tumor burden or condition required sacrifice and T_2 was found to be 5.6 ±1.9 days over an 11 day period culminating on the 24^{th} day following surgical implantation. Growth slowed for all tumors following irradiation, but at no point in the growth progression of large tumors was there a significant difference in size between the air and oxygen breathing groups (Fig. 4). Large tumors could only be monitored for about 20 days following irradiation, because the mean size was already 3.5 –4 cm^3 on the day of irradiation. The T_2 was found to be just over 12 days for both air and oxygen breathing rats.

Small tumors also continued to grow with no significant difference between air and oxygen breathing until day 13 (Fig. 4B). From day 13 onwards until the animals were sacrificed (post-irradiation day 25), the mean size of the small tumors in rats breathing oxygen was significantly smaller than those breathing air (Table 2). The ratios of these volumes ranged from 1.3 to 1.5 and might be loosely interpreted as an oxygen enhancement ratio (OER). Oxygen tension was measured in 6 large and 6 small tumors, but in one tumor of each type the pO_2 maps were of such poor quality (excessive errors in the estimates) that they were excluded from analysis involving pO_2. In addition, one rat from each type was sacrificed early (as per IACUC guidelines) due to tumor ulceration leaving four small and four large tumors for correlative oxygen analysis. For the Group of large tumors, two were found to be relatively well oxygenated (mean pO_2 > 10 torr) and two were poorly oxygenated (although in each case one breathed air and the other oxygen during irradiation). The response to irradiation was found to be very different depending on pO_2, as shown for the post irradiation growth curves (Fig. 5A). Both small and large tumors showed correlations (R2 > 0.8) between the mean pretreatment pO_2 and T_2 (Fig. 5B).

DISCUSSION

This investigation provides further evidence for the value and importance of measuring tumor oxygenation as a basis for predicting response to irradiation. In the preliminary experiment, we found that merely having rats with a range of R3327-AT1 tumor sizes breathe oxygen, before and during irradiation, had no significant effect on tumor growth delay. In the subsequent investigation stratification by tumor size revealed a modest, but significant benefit for small tumors, when rats breathed oxygen during a single dose of radiation, but groups of large tumors showed no benefit. However, pO_2 measurements indicated that regardless of tumor size better oxygenated tumors showed better response to irradiation. The results indicate correlations between pO_2 at time of irradiation and subsequent time to double in volume for both small and large tumors, irrespective of inhaled gas (Fig. 5A, B).

In common with our previous observations, the larger AT1 tumors were significantly more hypoxic and had lower mean and median pO_2 15, 21. Mean pO_2 in large tumors responded to hyperoxic gas breathing, but the hypoxic fraction resisted modulation rendering the tumors resistant to radiotherapy. Both groups of large tumors (4-air and -O_2) responded to irradiation with a significant reduction in growth rate: volume doubling time (VDT) reached 12 days post irradiation compared with a control VDT ~ 5 days. However, there was no benefit in terms of radiation response associated with oxygen breathing during irradiation for the groups of large AT1 tumors (Fig. 4, Table 2). However, the better oxygenated tumors showed better response to irradiation (Fig. 5A), and indeed, there was a correlation between time to double in volume (T_2) and pretreatment pO_2 in individual tumors (Fig. 5B). Thus, pO_2 measurements appear to

have prognostic value for this small cohort of tumors. A similar correlation was found previously in the slower growing and better differentiated Dunning prostate R3327-HI tumors [18].

For the smaller AT1 tumors, baseline pO_2 was generally significantly higher with only a small hypoxic fraction (HF_{10} <20%), which responded to hyperoxic gas breathing, as also observed previously [15, 21]. By day 4, the tumors in Group 5-O_2 were significantly smaller than controls and by day 7 both Groups 5-air and -O_2 showed significant growth delay compared with control tumors. After 13 days there was a significant effect of breathing oxygen and for all subsequent measurements tumors on oxygen breathing rats were significantly smaller than on air breathing rats (Fig. 4, Table 2). The continued increase in size following irradiation is in line with previous reports in similarly sized AT1 tumors with respect to single doses of X-rays [22]. Assessment of T_2 (the time to double in volume post irradiation) showed a linear relationship with pO_2 (Fig. 5B). However, the slope of the regression was very different for small and large tumors respectively. Smaller AT1 tumors have been reported to grow much faster than large AT1 tumors (VDT = 2.5 vs. 5.6 days) [23], but it is intriguing to note that the regression lines for small and large tumors appear to coincide for low pO_2. This may suggest an intrinsic growth rate and is similar to the growth expected for control non-irradiated tumors. Sauer *et al*. [24] previously examined the R3327-AT tumor and found a tendency towards greater hypoxia in larger tumors and greater DNA damage in the better oxygenated tumors as judged by the Comet assay.

The *FREDOM* approach provides measurements of pO_2 and in some ways is analogous to the Eppendorf Histograph or ESR (electron spin resonance) approaches based on particulate reporters. Each requires insertion of a needle into the tumor, but since HFB is a mobile liquid, we are able to use a particularly fine (32 gauge) needle. As with the Histograph, mean and median pO_2 and hypoxic fractions could be determined. Importantly, however, the hexafluorobenzene reporter molecules remain in the tumor for many hours allowing sequential measurements with respect to interventions [9]. Thus, the relative stability of baseline pO_2 could be observed (Fig. 3), as well as regional response to hyperoxic gas intervention (Figs. 2 and 3). By contrast, the Histograph requires new needle tracks for sequential measurements and very few studies have examined dynamic changes in pO_2 distributions in animal models [25] or attempted such measurements the clinic [26, 27]. Despite its invasiveness, the Histograph has been used in the clinic, particularly for accessible head and neck and cervical tumors and for limited studies in breast, brain and prostate [3, 28–30]. Measurements from multiple studies show strong predictive value for hypoxic fractions of cervical and head and neck tumors with respect to clinical outcome. Groups at both Dartmouth [31, 32] and Louvain [33–35], have exploited ESR with particulate reporters to assess tumor pO_2 dynamics. Although only a single location was interrogated within the tumor, O'Hara *et al.* [31] found a strong correlation between tumor growth rates and pre-therapy pO_2 in CALU-3 tumors undergoing radio immunotherapy, closely similar to our observations in Figure 5. O'Hara *et al.* [32] also showed that pO_2 measurements could be used to optimize timing of split dose radiotherapy..

The purpose of this study was to further evaluate the usefulness of NMR oximetry as a predictor of therapeutic outcome, so that tumor phenotypes (poorly) suited for oxygen manipulation may be identified in advance. A useful feature of the *FREDOM* technique is that it allows minimally invasive quantitative dynamic *in vivo* sampling of multiple regions within the tumor. Accordingly, tumors with a significant HF_{10} and more importantly those which resist therapeutic oxygen manipulation can be readily identified. In future clinical practice this could prompt application of hypoxia selective cytotoxins or radiation boost using IMRT [36, 37]. Of course, we recognize that this study used a single high dose of radiation and may be less pertinent to traditional fractionated regimens. Nonetheless, as the trend towards high dose stereotactic treatment develops, pO_2 measurements, as presented here, could become

increasingly pertinent and valuable. To date, the *FREDOM* approach could not be translated to the clinic due to lack of access to clinical ^{19}F MRI, but this is increasingly becoming available in major clinical centers. Moreover, extensive toxicological literature [38–40] does suggest that HFB could be used in patients once GMP (good manufacturing practice) is applied.

FREDOM has identified intrinsic differences in intratumoral oxygenation between the various sublines of Dunning R3327, and more importantly, the association between persistent hypoxia, and outcome following radiation therapy. We believe the demonstration of relevance to this second tumor line strengthens the rationale for further development and application of *FREDOM* with a view to ultimate clinical application.

Acknowledgements

We are grateful to Drs. Vikram Kodibagkar and Anca Constantinescu for collegial support. The research was supported in part by NIH RO1 CA79515/EB2762, a Predoctoral Training supplement R01 CA79515-S and the Cancer Imaging Program pre-ICMIC P20 CA86354. NMR experiments were performed at the Mary Nell & Ralph B. Rogers NMR Center an NIH BTRP # P41-RR02584.

References

1. Gray L, Conger A, Ebert M, et al. The concentration of oxygen dissolved in tissues at time of irradiation as a factor in radiotherapy. Br J Radiol 1953;26:638–648. [PubMed: 13106296]
2. Nordsmark M, Overgaard M, Overgaard J. Pretreatment oxygenation predicts radiation response in advanced squamous cell carcinoma of head and neck. Radiother Oncol 1996;41:31–39. [PubMed: 8961365]
3. Fyles AW, Milosevic M, Wong R, et al. Oxygenation predicts radiation response and survival in patients with cervix cancer. Radiother Oncol 1998;48:149–156. [PubMed: 9783886]
4. Brizel DM, Sibly GS, Prosmitz LR, et al. Tumor hypoxia adversely affects the prognosis of carcinoma of the head and neck. Int J Radiat Oncol Biol Phys 1997;38:285–289. [PubMed: 9226314]
5. Rofstad EK, Sundfor K, Lyng H, et al. Hypoxia-induced treatment failure in advanced squamous cell carcinoma of the uterine cervix is primarily due to hypoxia-induced radiation resistance rather than hypoxia-induced metastasis. Br J Cancer 2000;83:354–359. [PubMed: 10917551]
6. Coleman CN. Hypoxia in tumors: a paradigm for the approach to biochemical and physiological heterogeneity. J Natl Cancer Inst 1988;80:310–317. [PubMed: 3282077]
7. Höckel M, Vaupel P. Tumor Hypoxia: Definitions and Current Clinical, Biologic, and Molecular Aspects. J Natl Cancer Inst 2001;93:266–276. [PubMed: 11181773]
8. Overgaard J, Horsman MR. Modification of hypoxia-induced radioresistance in tumors by the use of oxygen and sensitizers. Semin Radiat Oncol 1996;6:10–21. [PubMed: 10717158]
9. Zhao D, Jiang L, Mason RP. Measuring Changes in Tumor Oxygenation. Methods Enzymol 2004;386:378–418. [PubMed: 15120262]
10. Stone HB, Brown JM, Phillips T, et al. Oxygen in human tumors: correlations between methods of measurement and response to therapy. Radiat Res 1993;136:422–434. [PubMed: 8278585]
11. Swartz, HM.; Dunn, JF. Measurements of oxygen in tissues: overview and perspectives on methods. In: Dunn, JF.; Swartz, HM., editors. Oxygen Transport to Tissue XXIV. 530. New York: Kluwer Academic; 2003. p. 1-12.
12. Foo SS, Abbott DF, Lawrentschuk N, et al. Functional imaging of intratumoral hypoxia. Molecular Imaging Biol 2004;6:291–305.
13. Mason RP, Ran S, Thorpe PE. Quantitative assessment of tumor oxygen dynamics: Molecular Imaging for Prognostic Radiology. J CellBiochem 2002;87(suppl):45–53.
14. Zhao D, Constantinescu C, Hahn EW, et al. Differential oxygen dynamics in two diverse Dunning prostate R3327 rat tumor sublines (MAT-Lu and HI) with respect to growth and respiratory challenge. Int J Radiat Oncol Biol Phys 2002;53:744–756. [PubMed: 12062621]
15. Zhao D, Ran S, Constantinescu A, et al. Tumor oxygen dynamics: correlation of in vivo MRI with histological findings. Neoplasia 2003;5:308–318. [PubMed: 14511402]

16. Zhao D, Jiang L, Hahn EW, et al. Tumor physiological response to combretastatin A4 phosphate assessed by MRI. Int J Radiat Oncol Biol Phys 2005;62:872–880. [PubMed: 15936572]
17. Xia M, Kodibagkar V, Liu H, et al. Tumour oxygen dynamics measured simultaneously by near infrared spectroscopy and ^{19}F magnetic resonance imaging in rats. Phys Med Biol 2006;51:45–60. [PubMed: 16357430]
18. Zhao D, Constantinescu A, Chang C-H, et al. Correlation of Tumor Oxygen Dynamics with Radiation Response of the Dunning Prostate R3327-HI Tumor. Radiat Res 2003;159:621–631. [PubMed: 12710873]
19. Hahn EW, Peschke P, Mason RP, et al. Isolated tumor growth in a surgically formed skin pedicle in the rat: A new tumor model for NMR studies. Magn Reson Imaging 1993;11:1007–1017. [PubMed: 8231664]
20. Peschke P, Hahn EW, Wenz F, et al. Differential sensitivity of three sublines of the rat Dunning prostate tumor system R3327 to radiation and/or local tumor hyperthermia. Radiat Res 1998;150:423–430. [PubMed: 9768856]
21. Mason RP, Constantinescu A, Hunjan S, et al. Regional tumor oxygenation and measurement of dynamic changes. Radiat Res 1999;152:239–249. [PubMed: 10453084]
22. Peschke P, Lohr F, Hahn E, et al. Response of the rat Dunning R3327-AT1 prostate tumor to treatment with fractionated fast neutrons. Radiat Res 1992;129:112–114. [PubMed: 1728053]
23. Lohr F, Wenz F, Flentje M, et al. Measurement of proliferative activity of three different sublines of Dunning rat prostate tumor R3327. Strahlenther Onkol 1993;169:438–445. [PubMed: 8342118]
24. Sauer G, Weber KJ, Peschke P, et al. Measuremment of hypoxia using the COMET assay correlates with preirradiation microelectrode pO_2 Histography in R3327-AT rodent tumos. Radiat Res 2000;154:439–446. [PubMed: 11023608]
25. Yeh KA, Biade S, Lanciano RM, et al. Polarographic Needle Electrode Measurements of Oxygen in Rat Prostate Carcinomas: Accuracy and Reproducibility. Int J Radiat Oncol Biol Phys 1995;33:111–118. [PubMed: 7642408]
26. Aquino-Parsons C, Green A, Minchinton AI. Oxygen tension in primary gynaecological tumours: the influence of carbon dioxide concentration. Radiother Oncol 2000;57:45–51. [PubMed: 11033188]
27. Falk S, Ward R, Bleehen N. The influence of carbogen breathing on tumor tissue oxygenation in man evaluated by computerized pO_2 histography. Br J Cancer 1992;66:919–924. [PubMed: 1419637]
28. Brizel DM, Scully SP, Harrelson JM, et al. Tumor oxygenation predicts for the likelihood of distant metastases in human soft tissue sarcoma. Cancer Res 1996;56:941–943. [PubMed: 8640781]
29. Höckel M, Schlenger K, Knoop C, et al. Oxygenation of carcinomas of the uterine cervix: evaluation by computerized O_2 tension measurements. Cancer Res 1991;51:6098–6102. [PubMed: 1933873]
30. Movsas B, Chapman JD, Hanlon AL, et al. Hypoxic prostate/muscle pO_2 ratio predicts for biochemical failure in patients with prostate cancer: preliminary findings. Urology 2002;60:634–639. [PubMed: 12385924]
31. O'Hara JA, Blumenthal RD, Grinberg OY, et al. Response to radioimmunotherapy correlates with tumor pO_2 measured by EPR oximetry in human tumor xenografts. Radiat Res 2001;155:466–473. [PubMed: 11182798]
32. O'Hara JA, Goda F, Demidenko E, et al. Effect on regrowth delay in a murine tumor of scheduling split-dose irradiation based on direct pO_2 measurements by electron paramagnetic resonance oximetry. Radiat Res 1998;150:549–556. [PubMed: 9806597]
33. Baudelet C, Gallez B. How does blood oxygen level-dependent (BOLD) contrast correlate with oxygen partial pressure (pO_2) inside tumors? Magn Reson Med 2002;48:980–986. [PubMed: 12465107]
34. Gallez B, Baudelet C, Jordan BF. Assessment of tumor oxygenation by electron paramagnetic resonance: principles and applications. NMR Biomed 2004;17:240–262. [PubMed: 15366026]
35. Gallez B, Jordan BF, Baudelet C, et al. Pharmacological modifications of the partial pressure of oxygen in murine tumors: Evaluation using in vivo EPR oximetry. Magn Reson Med 1999;42:627–630. [PubMed: 10502749]
36. Brown JM. Exploiting the hypoxic cancer cell: mechanisms and therapeutic strategies. Molec Med Today 2000;6:157–162. [PubMed: 10740254]

37. Webb S. Intensity-modulated radiation therapy (IMRT): a clinical reality for cancer treatment, “any fool can understand this”. The 2004 Silvanus Thompson Memorial Lecture. Br J Radiol 2005;78:S64–72. [PubMed: 16306638]

38. Courtney KD, Andrews JE. Teratogenic evaluation and fetal deposition of hexabromobenzene (HBB) and hexafluorobenzene (HFB) in CD-1 mice. J Environ Sci Health B 1984;19:83–94. [PubMed: 6715792]

39. Hall, LW.; Jackson, SRK.; Massey, GM. Hexafluorobenzene in veterinary anaesthesia. In: Arias, A.; Llaurado, R.; Nalda, MA., et al., editors. Recent Progress in Anaesthesiology and Resuscitation. Oxford: Excerpta Medica; 1975. p. 201-204.

40. Mortelmans KM, Simmon VF. *In vitro*microbiological mutagenicity assays of eight fluorocarbon taggant samples. Gov Rep Announce Index (US) 1981;81:2555–2587.

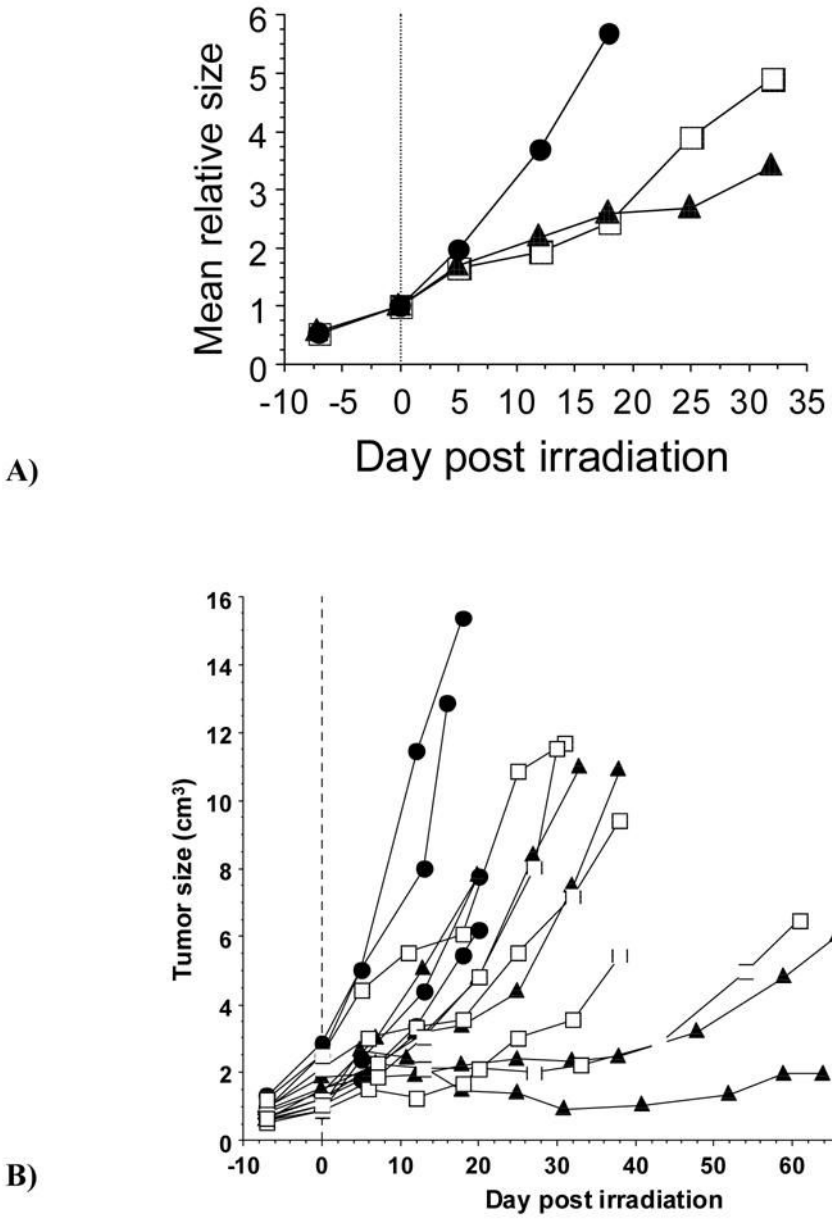

Figure 1. Influence of radiation on Dunning prostate R3327-AT1 tumor growth

A) Separate curves are shown for relative growth of sham irradiated tumors (n=4; ●) and those irradiated with single dose 30 Gy X-rays, while rats breathed air (n=5; □) or oxygen (n=5; ▲). There was no separation based on tumor size at time of irradiation.

B) Growth curves for the 14 individual tumors. ● sham irradiation, □ 30 Gy while breathing air, or ▲ oxygen. Absolute tumor sizes are shown relative to irradiation on day 0.

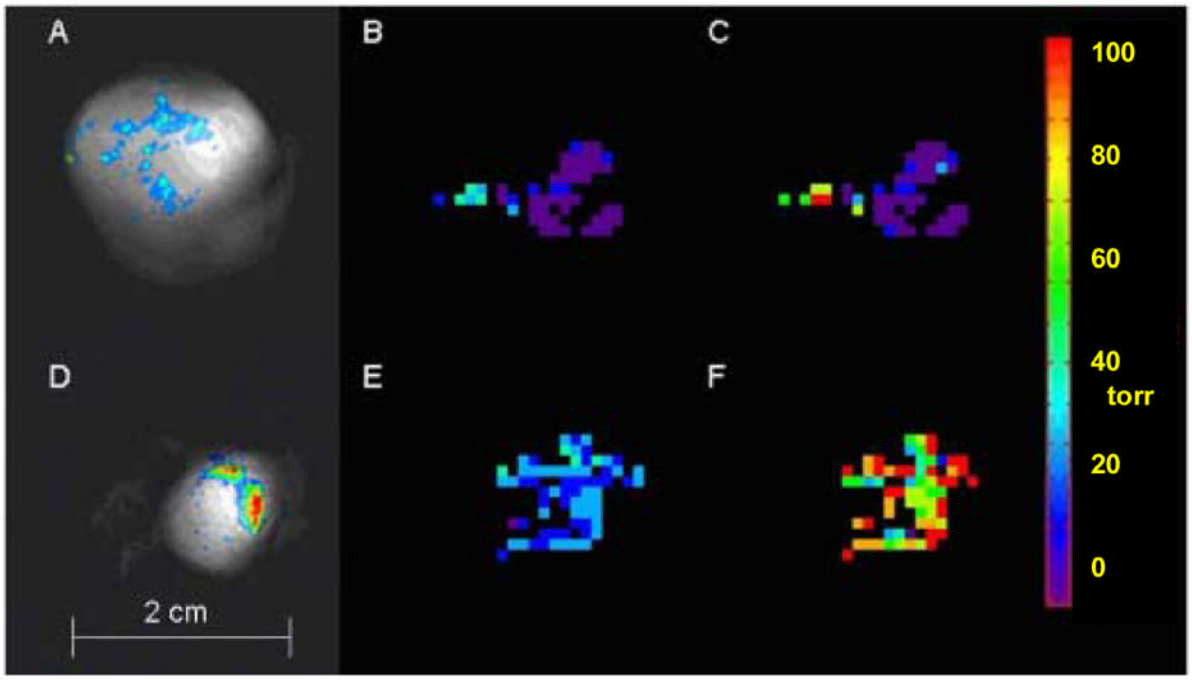

Figure 2. pO_2 maps obtained using *FREDOM* in two representative AT1 tumors

Upper images show a large tumor (3.6 cm^3) and lower images show a small tumor (1 cm^3).
A and D: Overlay of ^{19}F and ^{1}H NMR images shows HFB distribution. ^{19}F NMR signal to noise ratio = 27 for large tumor and 77 for small tumor with 51 and 100 acceptable voxels (pO_2 measurements), respectively.
B and E: Baseline pO_2 maps obtained with air breathing: mean pO_2= 0.1 ± 1.8 torr and 25.4 ± 1.1 torr respectively for large and small tumors.
C and F: pO_2 maps obtained after 24 minutes oxygen breathing, mean pO_2 = 8.1 ± 4.5 torr for large tumor, which was significantly different from baseline ($p<0.01$) and pO_2 = 90.6 ± 3.9 torr for small tumor which was significantly elevated ($p <0.0001$).

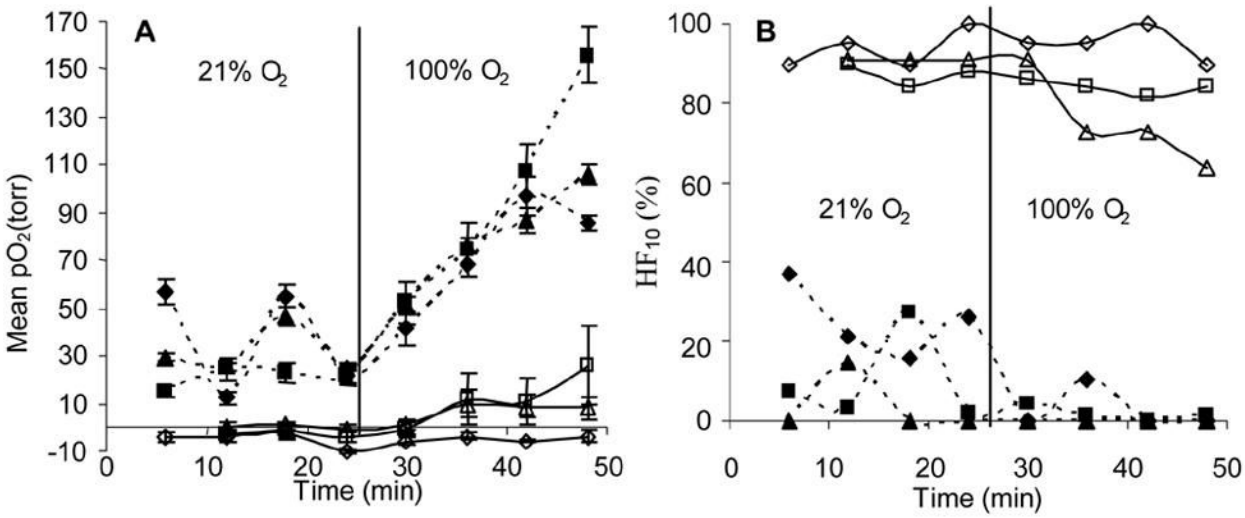

Figure 3. Changes in oxygenation and hypoxic fraction in response to oxygen inhalation

A: Mean ± SE pO_2 for each of three large (>3.0 cm^3, open symbols) and three small (<1.5 cm^3, solid symbols) tumors, obtained using sequential *FREDOM* scans.

B: Corresponding hypoxic fraction (HF_{10}) in the six tumors. The relatively small initial hypoxic fraction of the small tumors was essentially eliminated by oxygen inhalation, while the large tumors responded modestly.

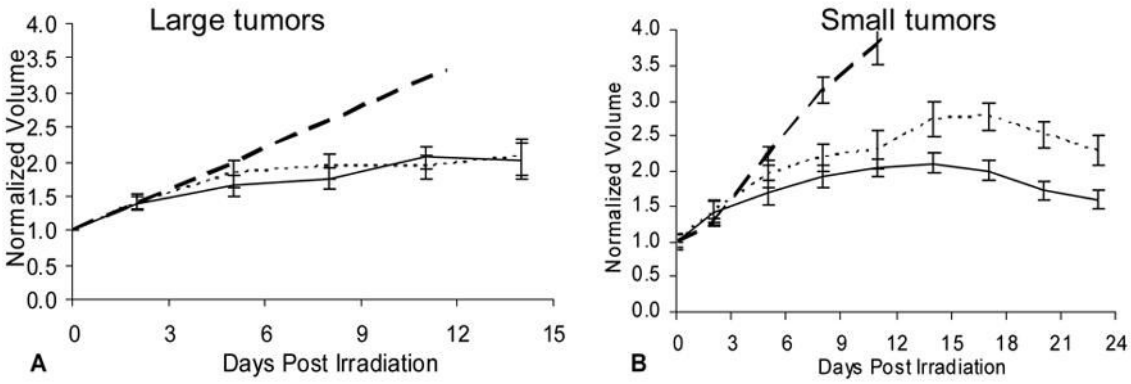

Figure 4. Tumor growth with respect to irradiation

Mean interpolated volume ± SE as a function of time, with each tumor normalized to its initial size at irradiation (Day 0).

A: For large AT1 tumors, no significant growth delay (α =0.05) was observed for tumors on oxygen breathing rats (solid) as compared to air breathing (dotted). Dashed line shows predicted growth of control tumors.

B: For small AT1 tumors, oxygen inhalation during irradiation (solid) resulted in a statistically significant ($p<0.001$) growth delay, which was evident by day 13 compared with air breathing rats (dotted). Both groups also showed significant delay compared with non-irradiated controls by day 7.

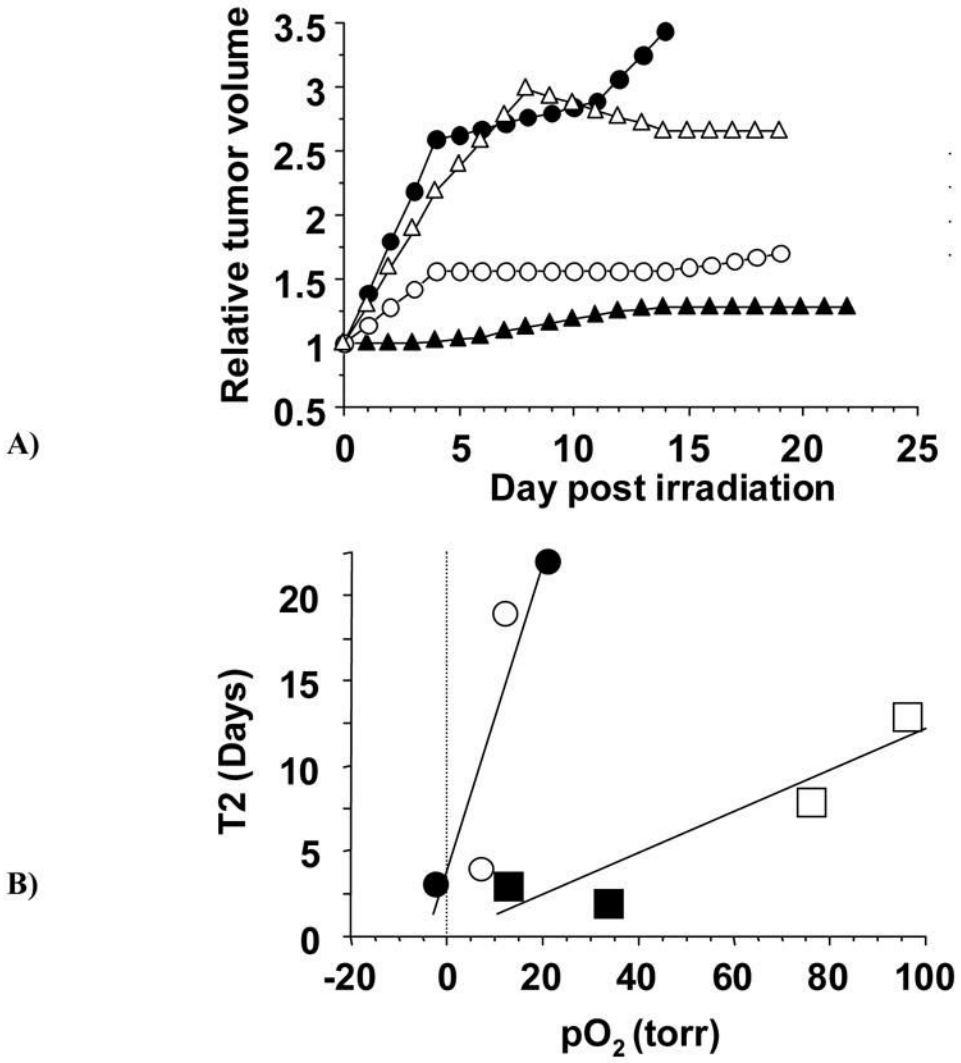

Figure 5. Influence of oxygen on tumor growth following irradiation

A: Growth of four large AT1 tumors following irradiation indicating different growth delays depending on pO_2. Those with solid symbols were on rats breathing air during irradiation, but had very different pO_2 values: ▲(pO_2 = 21 ± 2 (SE) torr) ● (pO_2 = −2.3 ± 0.6 torr (< 1 torr; p>0.99). Open symbols were on rats breathing oxygen during irradiation: o (pO_2 = 12 ± 5 torr) △ (pO_2 = 7 ± 2 torr).

B: Correlation between T2, the time to double in size following irradiation and pO_2 measured pretreatment. Separate curves are shown for small and large tumors, each of which shows a strong correlation (R2>0.8). Large tumors are shown as circles and small tumors as squares, open symbols for rats breathing oxygen and closed for air.

Table 1

Oxygen tension in R3327-AT1 Dunning prostate tumors for rats breathing air or oxygen

		Baseline (air)			Oxygen Inhalation		
		pO_2 (torr)			pO_2 (torr)		
Tumor Size	**No.**	**Mean +/− SE**	**Median**	**Mean HF_{10} (%)**	**Mean +/− SE**	**Median**	**Mean HF_{10} (%)**
Small (< 1.5 cm^3)	5	25.2 +/− 0.8	21.9 [a]	19.2 +/− 4.0			
Large (> 3.0 cm^3)	5	1.8 +/− 0.6 [*]	<9 [a]	77.8 +/− 8.5 [*]			
Oxygen challenged							
Small (< 1.5 cm^3: Group 5-O_2)	3 [^]	28.5 +/− 1.0	24.1	12.8 +/− 3.7	79.6 +/− 2.1 [‡]	74.4	1.4 +/− 0.9 [#]
Large (> 3.0 cm^3: Group 4-O_2)	3 [^]	−0.4 +/− 0.7 [*]	<6 [a]	91.0 +/− 1.3 [*]	4.9 +/− 1.6 [*]	<7 [a]	84.8 +/− 3.0 [*]

[*] p< 0.001 from small;

[‡] p< 0.001 from baseline;

[#] p< 0.01 from baseline

[^] a subset of the tumors above

[a] p> 0.95

Table 2

R3327-AT1 prostate tumor growth following irradiation for rats breathing air or oxygen during irradiation

Group	No.	Treatment	V_0 (cm^3) Mean +/− SE	T_2 (days) Mean +/− SE	V/V_0 Mean +/− SE	V/V_0 Mean +/− SE	V/V_0 Mean +/− SE	V/V_0 Mean +/− SE	V/Vo Mean +/− SE	V/Vo Mean +/− SE	V/Vo Mean +/− SE
Small (<1.5 cm^3)					*(Days 1-3)*	*(Days 4-6)*	*(Days 7-9)*	*(Days 10-12)*	*(Days 13-15)*	*(Days 16-18)*	*(Days 19-21)*
Group 3	6	Control	1.1 +/− 0.1	5.6 +/− 0.8	1.3 +/− 0.1	2.2 +/− 0.1	3.1 +/− 0.2	3.8 +/− 0.3	Sacrificed		
Group 5-air	6	30 Gy+ Air	0.7 +/− 0.1	9.3 +/− 3.4	1.4 +/− 0.1	2.0 +/− 0.2	2.2 +/− 0.2 ¶	2.3 +/− 0.2 ¶	2.7 +/− 0.3	2.8 +/− 0.3	2.5 +/− 0.2
						1.7 +/− 0.2 †	1.9 +/− 0.2 ‡	2.1 +/− 0.2 ‡			
Group 5-O_2	6	30 Gy + O_2	1.0 +/− 0.1	9.9 +/− 3.6	1.4 +/− 0.1				2.1 +/− 0.1 *	2.0 +/− 0.1 *	1.7 +/− 0.1 *
Large (>3.0 cm^3)					*(Days 1-3)*	*(Days 4-6)*	*(Days 7-9)*	*(Days 10-12)*	*(Days 13, 14)*		
Group 4-air	5	30 Gy+ Air	4.0 +/− 0.6	12.7 +/− 6.3	1.4 +/− 0.1	1.6 +/− 0.2	1.8 +/− 0.2	1.9 +/− 0.2	2.1 +/− 0.3		
Group 4-O_2	5	30 Gy + O_2	3.7 +/− 0.7	12.5 +/− 3.7	1.4 +/− 0.1	1.7 +/− 0.1	1.9 +/− 0.1	2.1 +/− 0.1	2.0 +/− 0.2		

Notes: V_O = Intial volume on treatment day, T_2 = Time to double V_O

* Significantly smaller than air breathing $p<0.05$

† Significantly smaller than controls $p<0.05$

‡ Significantly smaller than controls $p<0.0001$

¶ Significantly smaller than controls $p<0.0005$